

Nonlinear Position Controller Design for SynRM Drive Systems With Reduced Switching Frequency

Tian-Hua Liu*, Ming-Tsan Lin**, and You-Cheng Yang*

*Department of Electrical Engineering

National Taiwan University of Science and Technology

43, Section 4, Keelung Road

Taipei 106, Taiwan

**Department of Electrical Engineering

Tung-Nan Institute of Technology

Shen-Keng

Taipei 222, Taiwan

Abstract- This paper proposes a novel PWM switching method and control algorithm for synchronous reluctance drive systems. In this paper, first, in different switching modes, the current slope of the stator current can be systematically derived. The current slope is related to the dc-bus voltage, operating conditions, and parameters of the motor. Then, by computing the derivation of the current slope command and the real current slope, an optimum switching state can be determined and used to trigger the inverter. After that, the nonlinear controller for a position control system is proposed. By using the proposed method, the synchronous reluctance drive system performs very well. It has smaller current harmonics, lower switching frequency, and less switching loss when compared to the hysteretic current control. In addition, a fast transient response, good load disturbance rejection ability, and good tracking performance of position control can be achieved. No extra hardware is required. Several experimental results validate the theoretical analysis.

I. INTRODUCTION

The synchronous reluctance motor (SynRM) has been recognized to have many advantages due to its simple and rugged structure. In addition, the SynRM has no winding or magnetic material on its rotor. The SynRM is shown to be very suitable for ac drive systems due to many factors. First, the field-oriented control of the SynRM does not require computing slip frequency as required for the induction motor. As a result, there is no parameter sensitivity problem. Next, the SynRM does not require any permanent magnetic material as the permanent-magnet synchronous motor does.

To achieve a high performance drive system, the motor design, PWM switching strategy, and controller design are all important. Several researchers have studied and proposed many different techniques in these fields. In PWM techniques, the most popular method is the hysteretic or bang-bang current regulated control. This method is very simple; however, it provides a highly variable PWM switching frequency. In addition, its current ripple and harmonic content are large [1]. To solve the problem, the space vector modulation is proposed. The performance of the space vector modulation is excellent; nevertheless, this method requires a lot of complicated computations. As a result, a digital signal processor for space vector modulation is required [2]. Research on PWM strategies in induction motors or permanent magnet synchronous motors is popular; however, research on PWM

strategies of synchronous reluctance motor is not common. This has motivated us to study the PWM strategy for synRM drives. On the other hand, in the fields of motor drive and controller design, several techniques have been proposed for SynRM drives. For example, Vagati et al. proposed a flux-observer-based control scheme to achieve a high performance SynRM drive system [3]. Sul et al. developed a high dynamic torque control for a SynRM [4]. Liu et al. implemented an H^∞ to improve the dynamic response of a position control system for a SynRM [5]. These papers [3]-[5], however, only focus on linear controller design. To improve the performance of the SynRM drive system, nonlinear controllers are more effective and have been proposed. For example, Shyu et al. implemented a combination of the classical state feedback and the variable structure control [6]. The idea is good, however, the chattering problem appears in steady-state. Sul et al. proposed a nonlinear input-output linearization technique for an SynRM. The results achieved optimal efficiency. However, the computation of the control algorithm is very complicated [7].

In this paper, a novel PWM scheme for the SynRM is proposed to improve the torque response and reduce the switching frequency. The method is based on the measurement of the current slope. Although the computation is simple, the performance of the proposed method is satisfactory. Experimental results show that this method has a lower switching frequency, lower harmonics, and better current tracking ability. In addition, in order to improve the transient response, load disturbance rejection and tracking ability, a nonlinear controller is proposed here. To the best of the authors' knowledge, this is the first time the novel switching method and the nonlinear position controller for an SynRM drive system have been proposed. The details follow.

II. SWITCHING STRATEGY

2.1 Dynamic model of an SynRM

The mathematical model of a SynRM in d-q synchronous frame can be expressed as

$$\frac{di_d}{dt} = (\omega_e L_q i_q - r_s i_d + v_d) / L_d \quad (1)$$

and

$$\frac{di_q}{dt} = (-\omega_e L_d i_d - r_s i_q + v_q) / L_q \quad (2)$$

This paper is supported by the National Science Council, the R. O. C., through grant NSC 93-2213-E-011-012.

Where $\frac{d}{dt}$ is the differential operator, i_d is the d-axis current, i_q is the q-axis current, ω_e is the electrical speed, L_q is the q-axis inductance, L_d is the d-axis inductance, r_s is the stator resistance, v_d is the d-axis voltage, and v_q is the q-axis voltage. The electro-magnetic torque expressed in the d-q synchronous frame is

$$T_e = \frac{3}{2} \frac{P_0}{2} (L_d - L_q) i_d i_q = K_t i_q \quad (3)$$

where T_e is the electro-magnetic torque of the motor, P_0 is the number of poles of the motor, i_d is the d-axis equivalent current, i_q is the q-axis equivalent current, and K_t is the torque constant. The rotor speed and position of the motor can be expressed as

$$p \omega_r = \frac{1}{J} (T_e - T_l - B \omega_r) \quad (4)$$

and

$$p \theta_r = \omega_r \quad (5)$$

where J is the inertia constant of the motor and load, T_l is the external load torque, B is the viscous frictional coefficient of the motor and load, θ_r is the mechanical rotor position, and ω_r is the mechanical rotor speed. The electrical rotor speed and position are

$$\omega_e = \frac{P_0}{2} \omega_r \quad (6)$$

and

$$\theta_e = \frac{P_0}{2} \theta_r \quad (7)$$

where ω_e is the electrical rotor speed, and θ_e is the electrical rotor position of the motor.

2.2 Proposed switching Strategy

In this paper, a new switching strategy for the SynRM is proposed. The details are discussed here. If the inverter is switched in mode A⁺, the switching state is (1, 0, 0). Then, the dynamic equations of the d-q axis currents are expressed as:

$$\left. \frac{di_d}{dt} \right|_{\text{modeA}^+} = \frac{\omega_e L_q i_q - r_s i_d}{L_d} + \frac{2}{3} \frac{V_{dc} \sin \theta_e}{L_d} \quad (8)$$

and

$$\left. \frac{di_q}{dt} \right|_{\text{modeA}^+} = -\frac{\omega_e L_d i_d - r_s i_q}{L_q} + \frac{2}{3} \frac{V_{dc} \cos \theta_e}{L_q} \quad (9)$$

When the inverter is switched in a zero-voltage mode (free-wheeling mode), the switching state is (1, 1, 1) or (0, 0, 0). Then, the motor is three-phase shorted and is disconnected with the input voltage. The input voltage, therefore, is equal to zero. By substituting $V_{dc} = 0$ into equations (8)-(9), one can obtain

$$\left. \frac{di_d}{dt} \right|_{\text{mode}e0} = \frac{\omega_e L_q i_q - r_s i_d}{L_d} \quad (10)$$

$$\left. \frac{di_q}{dt} \right|_{\text{mode}e0} = -\frac{\omega_e L_d i_d - r_s i_q}{L_q} \quad (11)$$

Combining (8)-(11), one can easily obtain

$$\left. \frac{di_d}{dt} \right|_{\text{modeA}^+} = \left. \frac{di_d}{dt} \right|_{\text{mode}e0} + \frac{2}{3} \frac{V_{dc} \sin \theta_e}{L_d} \quad (12)$$

$$\left. \frac{di_q}{dt} \right|_{\text{modeA}^+} = \left. \frac{di_q}{dt} \right|_{\text{mode}e0} + \frac{2}{3} \frac{V_{dc} \cos \theta_e}{L_q} \quad (13)$$

By using the same method, one can derive that the switching mode B⁺ and C⁺ have the following dynamic equations:

$$\left. \frac{di_d}{dt} \right|_{\text{mode}eB^+} = \left. \frac{di_d}{dt} \right|_{\text{mode}e0} + \frac{2}{3} \frac{V_{dc} \sin(\theta_e - \frac{2\pi}{3})}{L_d} \quad (14)$$

$$\left. \frac{di_q}{dt} \right|_{\text{mode}eB^+} = \left. \frac{di_q}{dt} \right|_{\text{mode}e0} + \frac{2}{3} \frac{V_{dc} \cos(\theta_e - \frac{2\pi}{3})}{L_q} \quad (15)$$

and

$$\left. \frac{di_d}{dt} \right|_{\text{mode}eC^+} = \left. \frac{di_d}{dt} \right|_{\text{mode}e0} + \frac{2}{3} \frac{V_{dc} \sin(\theta_e + \frac{2\pi}{3})}{L_d} \quad (16)$$

$$\left. \frac{di_q}{dt} \right|_{\text{mode}eC^+} = \left. \frac{di_q}{dt} \right|_{\text{mode}e0} + \frac{2}{3} \frac{V_{dc} \cos(\theta_e + \frac{2\pi}{3})}{L_q} \quad (17)$$

To realize the proposed method, first we measure the current slope in the free-wheeling switching state. Then, we compute the desired d-axis current slope between the current command i_d^* and the real current i_d , and the desired q-axis current slope between the current command i_q^* and the real current i_q , which are expressed as:

$$\left(\frac{di_d}{dt} \right)^* = \frac{i_d^* - i_d}{T} \quad (18)$$

and

$$\left(\frac{di_q}{dt} \right)^* = \frac{i_q^* - i_q}{T} \quad (19)$$

where $\left(\frac{di_d}{dt} \right)^*$ is the desired current slope, and T is the switching interval of the inverter. After that, we can compute

the current deviation between the desire current slope and the current slope at mode 0:

$$\Delta i_d = \left(\left(\frac{di_d}{dt} \right)^* - \frac{di_d}{dt} \Big|_{mode0} \right) T \quad (20)$$

and

$$\Delta i_q = \left(\left(\frac{di_q}{dt} \right)^* - \frac{di_q}{dt} \Big|_{mode0} \right) T \quad (21)$$

The required voltage vector angle is

$$\gamma = -\tan^{-1} \left(\frac{L_d \Delta i_d}{L_q \Delta i_q} \right) + \theta_e \quad (22)$$

Finally, the voltage vector of the inverter can be selected according to the vector angle γ . In Fig. 1, for example, the vector V_6 is selected when γ is between -30° and 30° . In the real world, if the required voltage amplitude is small, we choose a free-wheeling voltage vector to reduce the current harmonics.

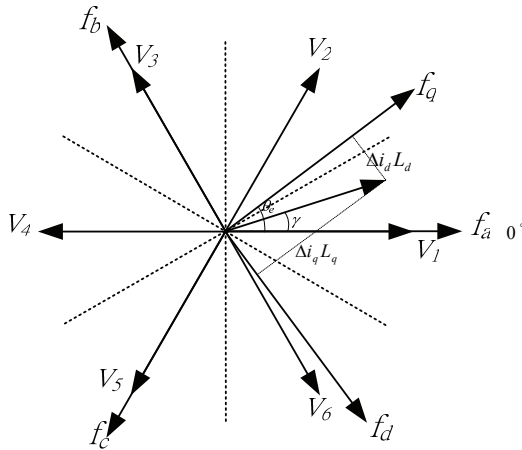


Fig. 1 The selected voltage vector.

III. NONLINEAR CONTROLLER DESIGN

Many papers have proposed different control methods to improve the dynamic performance of synchronous reluctance drive systems. For example, Thanaa et al. proposed a sliding mode controller for position control of a vector-controlled synchronous reluctance drive system. The results are satisfactory; however, the control method requires knowing the parameter variation bounds of the motor. In addition, a boundary layer is required to alleviate the chattering problem [8]. Lee et al. used the feedback linearization technique to obtain an efficiency-optimized direct torque control. The idea is of great interest; however, the controller is very complicated and requires a lot of computation [7]. Liu et al. proposed an H^∞ controller to improve the transient response and load disturbance response of a position control system for a synchronous reluctance motor. The experimental results are satisfactory; however, the controller is complicated [9]. Chiang et al. proposed an

integral variable structure controller with grey prediction for a synchronous reluctance drive system. The method can significantly reduce chattering and steady-state error; however, the control method requires a lot of computing time using a digital signal processor [10]. Recently, Shyu et al. proposed a state feedback controller combined with a variable structure controller for position controller of a synchronous reluctance motor. The idea is new and interesting; however, a chattering problem exists due to the high frequency switching of the variable structure controller [11].

In order to reduce the complication of the controllers mentioned above [7]-[11], this paper proposes a simple nonlinear controller for a SynRM drive system. Only the error signal is used here. By combining the integral and proportional items of the error signal and its nonlinear operation, a control input u can be obtained. A systematic stability analysis of the control system is discussed. The proposed method can be applied for a speed control system and a position control system. To the authors' best knowledge, this is the first time that the proposed method has been applied to a SynRM drive system. The details are shown as follows.

The block diagram of the closed-loop position control system is shown in Fig. 2. From Fig. 2, we can obtain

$$i_q^* = K_p (\omega_r^* - K_v \omega_r) \quad (23)$$

By substituting (23) into (3) and (4), we can derive

$$\dot{\omega}_r = \frac{K_t}{J} K_p (\omega_r^* - K_v \omega_r) - \frac{T_L}{J} \quad (24)$$

Define the position error as

$$e_\theta = \theta_r^* - \theta_r \quad (25)$$

By taking the derivative of equation (25), we can obtain

$$\dot{e}_\theta = \dot{\theta}_r^* - \dot{\theta}_r \quad (26)$$

To obtain a nonlinear position controller, the control input of the position control system is selected as

$$u = G_{ep} \frac{\partial V(e_\theta, \omega_r)}{\partial e_\theta} + G_{ip} \int \frac{\partial V(e_\theta, \omega_r)}{\partial e_\theta} dt + G_{xp} \frac{\partial V(e_\theta, \omega_r)}{\partial \omega_r} \quad (27)$$

where G_{ep} is the proportional gain of the position-loop controller, G_{ip} and G_{xp} are the integral gain of the position-loop controllers.

In this paper, the Lyapunov function of the position control system is selected as [12]:

$$V(e, \omega_r) = \frac{3}{4} K_{p0} e_\theta^4 + \frac{1}{2} K_{p1} e_\theta^2 + \frac{3}{4} K_{i0} e_\theta^4 + \frac{1}{2} K_{i1} e_\theta^2 + \frac{1}{2} K_{x0} \omega_r^2 \quad (28)$$

Substituting (28) into (27), we can obtain

$$u = G_{ep} (K_{p0} + K_{i0}) e_\theta^{\frac{1}{3}} + G_{ep} (K_{p1} + K_{i1}) e_\theta + G_{xp} (K_{p0} + K_{i0}) \int e_\theta^{\frac{1}{3}} dt +$$

$$G_{ip}(K_{p1} + K_{i1}) \int e_{\theta} dt + G_{xp} K_{x0} \omega_r \quad (29)$$

In order to simplify the expression of (29), we define

$$K_{pnr} = G_{ep}(K_{p0} + K_{i0}) \quad (30)$$

$$K_{per} = G_{ep}(K_{p1} + K_{i1}) \quad (31)$$

$$K_{inr} = G_{ip}(K_{p0} + K_{i0}) \quad (32)$$

$$K_{ier} = G_{ip}(K_{p1} + K_{i1}) \quad (33)$$

and

$$K_{xpr} = G_{xp} K_{x0} \quad (34)$$

By substituting (30)-(34) into (29), we can derive the control input as

$$u = \omega_r^* = K_{pnr} e_{\theta}^{\frac{1}{3}} + K_{per} e_{\theta} + K_{inr} \int e_{\theta}^{\frac{1}{3}} dt + K_{ier} \int e_{\theta} dt + K_{xpr} \omega_r \quad (35)$$

After that, the Lyapunov theorem is used to validate the stability of the position control system. We can take the derivation of the Lyapunov function and express it as

$$\dot{V}(e, \omega_r) = (K_{p0} + K_{i0}) e_{\theta}^{\frac{1}{3}} \dot{e}_{\theta} + (K_{p1} + K_{i1}) e_{\theta} \dot{e}_{\theta} + K_{x0} \omega_r \dot{\omega}_r \quad (36)$$

By substituting (24) and (26) into (36), and doing some mathematical process, we can obtain

$$\begin{aligned} \dot{V}(e, \omega_r) = & -(K_{p0} + K_{i0}) e_{\theta}^{\frac{1}{3}} \dot{\omega}_r - (K_{p1} + K_{i1}) e_{\theta} \dot{\omega}_r + K_{x0} \left[\frac{K_p K_t}{J} (K_{pnr} e_{\theta}^{\frac{1}{3}} \omega_r + \right. \\ & \left. K_{per} e_{\theta} \omega_r + K_{inr} \omega_r \int e_{\theta}^{\frac{1}{3}} dt + K_{ier} \omega_r \int e_{\theta} dt + K_{xpr} \omega_r^2 - K_v \omega_r^2) - \frac{T_L \omega_r}{J} \right] \quad (37) \end{aligned}$$

Next, by choosing

$$K_{x0} = \frac{J}{K_p G_{ep} K_t} \quad (38)$$

Then, substituting (38) into (37), we can obtain

$$\dot{V}(e, \omega_r) = \frac{1}{G_{ep}} (K_{inr} \omega_r \int e_{\theta}^{\frac{1}{3}} dt + K_{ier} \omega_r \int e_{\theta} dt + K_{xpr} \omega_r^2 - K_v \omega_r^2 - \frac{T_L \omega_r}{K_p K_t}) \quad (39)$$

In this paper, we select

$$K_v > \left| K_{inr} \int e_{\theta}^{\frac{1}{3}} dt + K_{ier} \int e_{\theta} dt + K_{xpr} + \frac{T_L}{K_p K_t} \right| \quad (40)$$

Substituting (40) into (39), we can obtain

$$\begin{aligned} \dot{V}(e, \omega_r) = & \frac{1}{G_{ep}} \left(- \left| K_{inr} \int e_{\theta}^{\frac{1}{3}} dt \right| \omega_r^2 + K_{inr} \omega_r \int e_{\theta}^{\frac{1}{3}} dt - \left| K_{ier} \int e_{\theta} dt \right| \omega_r^2 \right. \\ & \left. + K_{ier} \omega_r \int e_{\theta} dt - \left| \frac{T_L \omega_r}{K_p K_t} \right| \omega_r^2 - \frac{T_L \omega_r}{K_p K_t} \right) \leq 0 \quad (41) \end{aligned}$$

Define

$$Z_1(t) = \frac{1}{G_{ep}} (K_{inr} \omega_r \int e_{\theta}^{\frac{1}{3}} dt + K_{ier} \omega_r \int e_{\theta} dt + K_{xpr} \omega_r^2 - K_v \omega_r^2 - \frac{T_L \omega_r}{K_p K_t}) \leq 0 \quad (42)$$

By integrating (42), we can derive

$$\int_0^t z_1(\tau) d\tau = V(e(t), \omega_r(t)) - V(e(0), \omega_r(0)) \quad (43)$$

Because $e(t)$ and $\omega_r(t)$ are bounded, from equation (43), we can obtain

$$\lim_{t \rightarrow \infty} \int z_1(\tau) d\tau < \infty \quad (44)$$

Because $z_1(t)$ and $\dot{z}_1(t)$ are bounded, and $z_1(t)$ is a uniform and continuous function. From Barbalet's lemma, we can obtain

$$\lim_{t \rightarrow \infty} z_1(t) = 0 \quad (45)$$

Combining (41) and (45), we can conclude that the proposed position control system converges to a zero steady-state error. As a result, the position control system is an asymptotically stable system.

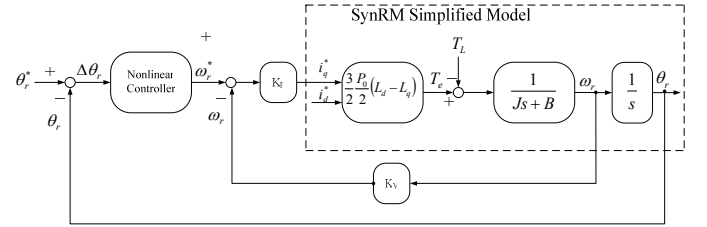


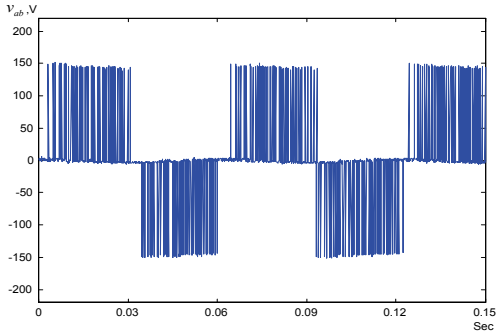
Fig. 2 The block diagram of the proposed system

IV. EXPERIMENTAL RESULTS

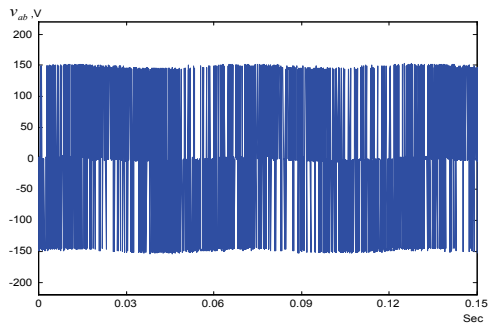
The proposed system uses a 32-bit digital signal processor, TMS 320C30, to determine the PWM switching states and execute the control algorithms. The dc bus voltage of the inverter is 150V. The sampling interval of the current-loop is 100 μ s, and the sampling intervals of the velocity- and position-loop are 1ms, respectively. The motor is a 3-phase, 4 pole, rated speed 1800 r/min, 0.75hp. It was manufactured by the Reliance Electric Company. Several experimental results are shown here. Fig. 3 (a)(b) show the measured line-to-line voltage of the motor. Fig. 3(a) is the result of the proposed PWM control. Fig. 3(b) is the waveform of the bang-bang PWM control. As you can observe, the proposed PWM method has a lower switching frequency than the traditional bang-bang control. Fig. 4(a)(b) show the measured a-phase currents of the motor. Fig. 4(a) is the current waveform of the proposed control method and Fig. 4(b) is the waveform of the bang-bang control. The proposed method has lower harmonics than the bang-bang control. Fig. 5(a)(b) compare the switching conditions of the proposed method and bang-bang control. Fig. 6 shows the tracking performance of the torque. Again, the proposed method performs better than the bang-bang control although the proposed method has a lower switching frequency than the traditional bang-bang control.

Fig. 7 (a)(b) show the measured responses of position and velocity of the nonlinear controller as the shaft of the

motor is controlled from 180 degrees to -180 degrees. Fig. 8 shows the load disturbance position response when a 2 N.m load is added. Fig. 9 shows the measured sinusoidal position responses of the nonlinear controller. It performs satisfactory again.

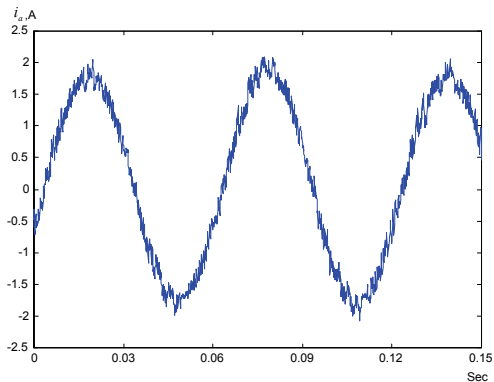


(a)

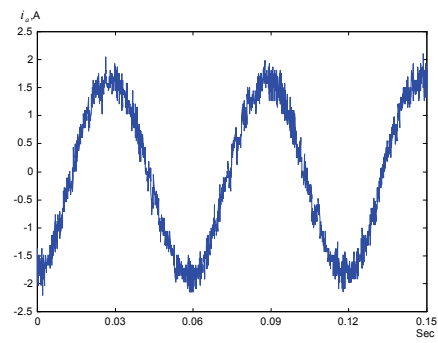


(b)

Fig. 3 the voltage v_{ab} (a)proposed (b)bang-bang.

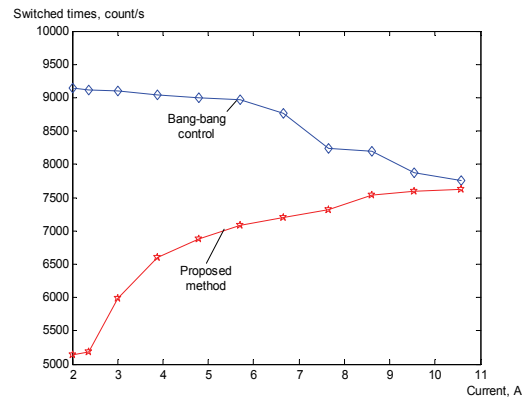


(a)

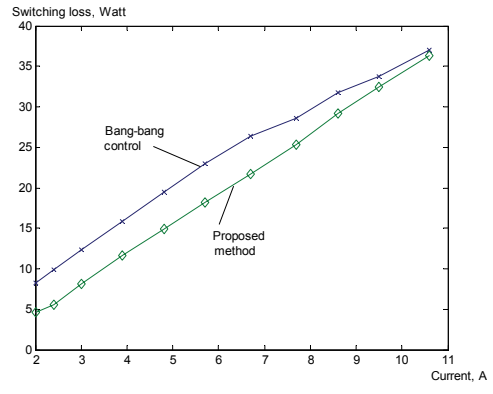


(b)

Fig. 4 the current i_a (a) proposed (b) bang-bang.



(a)



(b)

Fig. 5 The switching conditions to different load. (a)switching frequency (b)switching loss.

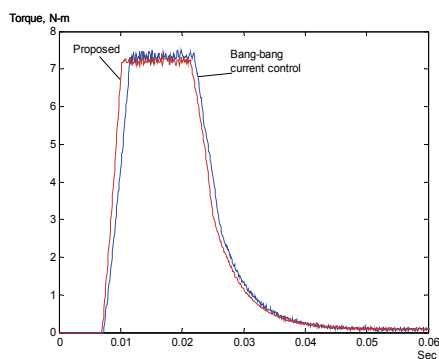
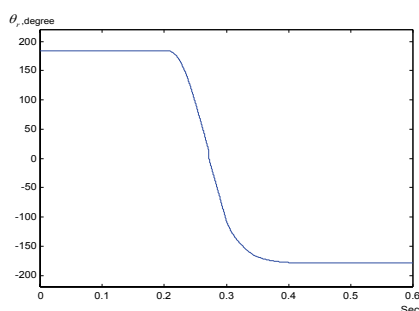
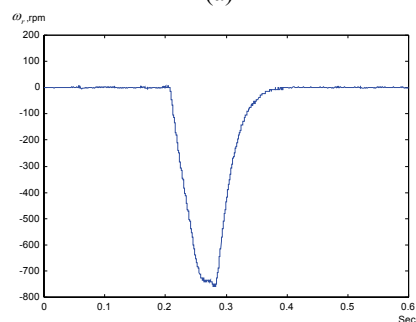


Fig. 6 The torque responses.



(a)



(b)

Fig. 7 The measured transient position responses (a) position (b) velocity.

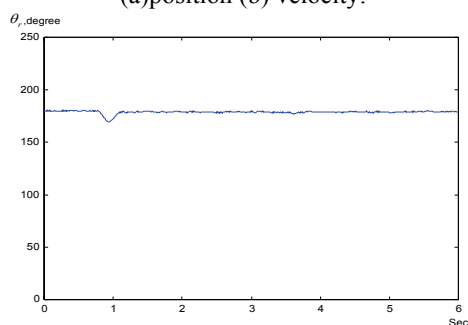


Fig. 8 The measured load disturbance response.

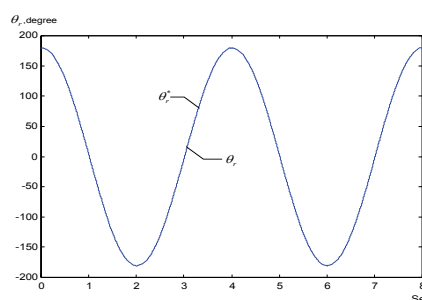


Fig. 9 The measured sinusoidal position responses

VI. CONCLUSIONS

In this paper, a new PWM strategy and a novel control algorithm are proposed. The PWM strategy and the control algorithm are implemented by a 32-bit digital signal processor. As a result, the hardware is very simple and a fully digital control system is achieved. In addition, the proposed method can be applied to a position control system. Experimental results show that the proposed system has satisfactory performance and can be applied to a synchronous reluctance drive system.

REFERENCES

- [1] M. P. Kazmierkowski and L. Malesani, "Current control techniques for three-phase voltage-source PWM converters: a survey", *IEEE Trans. Ind. Electron.*, vol. 45, no. 5, Oct. 1998, pp. 691-703.
- [2] J. Holtz and B. Bayer, "Fast current trajectory tracking control based on synchronous optimal pulsewidth modulation", *IEEE Trans. Ind. Appl.*, vol. 31, no. 5, Sep./Oct. 1995, pp. 1110-1112.
- [3] A. Vagati, M. Pastorelli, and G. Franceschini, "High-performance control of synchronous reluctance motors", *IEEE Trans. Ind. Appl.*, vol. 33, no. 4, July/Aug. 1997, pp. 983-991.
- [4] S. J. Kang and S. K. Sul, "Highly dynamic torque control of synchronous reluctance motor", *IEEE Trans. Power Electron.*, vol. 13, no. 4, July 1998, pp. 793-798.
- [5] M. T. Lin and T. H. Liu, "Design and implementation for a digital synchronous reluctance drive", *IEEE Trans. Aerospace and Electron. Syst.*, vol. 34, no. 4, Oct. 1998, pp. 1149-1164.
- [6] K. K. Shyu and C. K. Lai, "Incremental motion control of synchronous reluctance motor via multisegment sliding mode control method", *IEEE Trans. Control Systems Technology*, vol. 10, no. 2, Mar. 2002, pp. 169-176.
- [7] H. D. Lee, S. J. Kang, and S. K. Sul, "Efficiency-optimized direct torque control of synchronous reluctance motor using feedback linearization", *IEEE Trans. Ind. Electron.*, vol. 46, no. 1, Feb. 1999, pp. 192-198.
- [8] S. E. Thanaa, W. D. Matthew, E. F. John, and W. W. Barry, "Nonlinear robust control of a vector-controlled synchronous reluctance machine", *IEEE Trans. Power Electron.*, vol. 14, no. 6, Nov. 1999, pp. 1111-1121.
- [9] M. S. Lin and T. H. Liu, "Design and implementation of a robust controller for a synchronous reluctance drive", *IEEE Trans. Aerospace Electron. Syst.*, vol. 37, no. 4, Oct. 1999, pp. 1344-1358.
- [10] H. K. Chiang and C. H. Tseng, "Integral variable structure controller with grey prediction for synchronous reluctance motor drive", *IEE Proc.-Electr. Power Appl.*, vol. 151, no. 3, May 2004, pp. 349-358.
- [11] K. K. Shyu, C. K. Lai, and J. Y. Hung, "Totally invariant state feedback controller for position control of synchronous reluctance motor", *IEEE Trans. Ind. Electron.*, vol. 48, no. 3, June 2001, pp. 615-624.
- [12] S. E. Lyshevski, *Control Systems Theory with Engineering Applications*, Birkhauser, Boston: 2001.